Published in final edited form as:
Neuroscience. 2010 June 30; 168(2): 498–504. doi:10.1016/j.neuroscience.2010.03.037.

Projections from ventral hippocampus to medial prefrontal cortex but not nucleus accumbens remain functional after fornix lesions in rats

Richard L. Saint Marie, **Ethan J. Miller**, **Michelle R. Breier**, **Martin Weber**, and **Neal R. Swerdlow**
Department of Psychiatry, University of California San Diego, La Jolla, CA

Abstract

Sensorimotor gating, as measured by prepulse inhibition (PPI) of startle, is deficient in humans with schizophrenia and is greatly reduced in rats after bilateral infusion of N-methyl-D-aspartate (NMDA) into the ventral hippocampus (VH). The disruption of PPI by bilateral VH NMDA infusion is blocked by bilateral medial prefrontal cortex (mPFC) lesions, but not by bilateral lesions of the fornix, which is the principal output pathway of the hippocampal formation of the VH. Tract-tracing studies have demonstrated the presence of additional "non-fornical" pathways by which the VH and neighboring structures of the amygdala may reach forebrain regions that regulate PPI, including the mPFC. To determine whether these non-fornical pathways might mediate forebrain activation after VH NMDA infusion, we examined the effects of bilateral VH NMDA infusion on c-Fos protein expression in the mPFC and nucleus accumbens (NAC) after sham vs. bilateral fornix lesions. Significant elevations of c-Fos expression were observed in both the mPFC and NAC after bilateral VH NMDA infusions. Fornix lesions blocked enhanced c-Fos expression in the NAC but not the mPFC after VH NMDA infusion. The results suggest that an intact fornix may be necessary for VH activation of the NAC, but that the VH utilizes additional non-fornical projections to activate PPI-regulatory circuits within the mPFC.

Keywords

c-Fos; N-methyl-D-aspartate; prepulse inhibition; schizophrenia; sensorimotor gating

INTRODUCTION

Prepulse inhibition (PPI) is an operational measure of sensorimotor gating, in which a weak lead stimulus inhibits the motor response to an intense, startling stimulus (Graham 1975). PPI in laboratory animals has been used to understand the neural and genetic basis for PPI deficits in several neuropsychiatric disorders. PPI is potently regulated by limbic-cortical circuitry in rats, including portions of the ventral hippocampal region (VH), and this regulation has been studied to understand the potential contribution of VH pathology to PPI deficits in schizophrenia patients (Braff et al. 1978; cf. Swerdlow et al. 2008). As per Witter and Amaral

Correspondence: Neal R. Swerdlow, M.D., Ph.D., Department of Psychiatry, UCSD School of Medicine, 0804, 9500 Gilman Drive, La Jolla, Ca 92093-0804, Phone 619-543-6270, FAX 619-543-2493, nswerdlow@ucsd.edu.

(2004), the ventral "hippocampal region" refers to the hippocampal formation (dentate gyrus, hippocampus (CA1, CA2 and CA3), and subiculum) and parahippocampal region (entorhinal, perirhinal and postrhinal cortices and pre- and parasubicula).

Our group and others have endeavored to identify efferent projections from the VH to ventral forebrain targets - including the nucleus accumbens (NAC) and medial prefrontal cortex (mPFC) - that might mediate the loss of PPI after acute hippocampal activation, e.g. via intra-VH infusion of N-methyl-D-aspartate (NMDA) (Wan et al. 1996). Based on the potent regulation of PPI by the NAC (Swerdlow et al., 1986; cf. Swerdlow et al. 2001a, 2008) and the known interplay of the VH and NAC in the regulation of other behaviors in rats (e.g. Mogenson and Nielsen, 1984), a parsimonious explanation was that the PPI-regulatory effects of the VH were mediated by projections to the NAC via the fimbria/fornix, the main fiber tract exiting the VH. This explanation was not easily reconciled with our observation that the PPI-disruptive effects of intra-VH NMDA infusion remained intact after transection of the fornix (Swerdlow et al. 2004), but were opposed by electrolytic lesions of the mPFC (Shoemaker et al. 2005a). Rather, these findings suggested that non-fornical projections from the VH to the mPFC might mediate the PPI-disruptive effects of intra-VH NMDA infusion.

In a series of fiber-tracing studies (Miller et al. 2010), we then demonstrated that projections from portions of the VH (e.g., the lateral entorhinal cortex) and the embedded olfactory and vomeronasal parts of the amygdala to the mPFC remained intact after electrolytic ablation of the fornix in male Sprague Dawley rats. Conceivably, these projections might be responsible for the fact that the PPI-disruptive effects of VH activation persist after fornix lesions. While these fiber tracing studies document the presence of these projections, they do not demonstrate that these particular projections remain functional, i.e. capable of modifying mPFC function (and thereby conceivably PPI) and are activated by intra-VH NMDA infusion after fornix lesions. The present studies tested whether NMDA infusion into the VH causes physiological evidence of activation in the mPFC after fornix ablation.

EXPERIMENTAL PROCEDURES

Experimental Animals

Adult male Sprague-Dawley rats (n = 56; 225–250 g; Harlan, Livermore, USA) were housed in groups of 2–3 and maintained on a reversed 12-h light/dark schedule with *ad libitum* food and water. Rats were handled individually within 2 days of arrival and surgeries occurred 6–8 days after arrival. Care was taken to minimize animal suffering and reduce the number of animals used. Experiments conformed to guidelines of the National Institutes of Health for the use of animals in biomedical research (NIH Publication No. 80-23) and were approved by the Animal Subjects Committee at the University of California, San Diego (Protocol S01221).

Surgical Preparations and NMDA Infusions

Rats were administered 0.1 ml atropine (Vedco, 0.054 mg/ml) subcutaneously 15–30 min prior to being anesthetized using sodium pentobarbital (Nembutal, Abbot, 60 mg/kg, i.p.) and were then placed in a Kopf stereotaxic instrument in the flat-brain position (tooth bar 3.3 mm below the interaural line). Bilateral 23 gauge guide cannulae (10 mm) were aimed 3 mm above the VH at coordinates: AP −6.0, L ±5.4, DV −5.1 relative to Bregma (infusion needles were designed to extend 3 mm from the base of the guide cannulae – ultimate DV coordinate −8.1). Cannulae were anchored to the skull with cement and screws, surrounded by a plastic cap and filled with wire stylets. Initially (Experiment A), 8 rats were cannulated bilaterally to confirm the positive effects of VH NMDA vs. vehicle infusion on c-Fos expression in the mPFC and NAC, as reported by Klarner et al. (1998). In a separate experiment (B), 48 rats were cannulated bilaterally and 26 of these received bilateral electrolytic lesions of the fornix (AP −1.6, L ±1.7,

DV −5.0 relative to Bregma) by twice passing a 2.0 mA × 15 s current (Ugo Basile, 3500 Lesion Producing Device, Varese, Italy). The remaining rats received no lesion, i.e., no puncture of the brain or skull other than those for the VH cannulae. Seven to 9 days later, rats were brought to the laboratory and allowed to acclimate for at least 2 h. They were then infused bilaterally with NMDA (0.8 μg/0.5μl/side) or vehicle (normal saline), balanced for lesion condition, and allowed to rest quietly for an additional 2 hrs. Rats were then deeply anesthetized with sodium pentobarbital (Fatal Plus, Vortek Pharmaceuticals, 0.4 ml i.p., 390 mg/ml) and perfused intra-aortically with normal saline (1 min) followed by freshly made para-formaldehyde (4% in 0.08 M phosphate buffer, 2.5 min). These experimental parameters were selected based on our published evidence of: 1) effective disruption of PPI that is spared after fornix lesions (VH cannulae, NMDA infusion; e.g. Wan et al. 1996; Swerdlow et al. 2004); and 2) anatomical evidence of disruption of VH-NAC projections (fornix lesions; Miller et al. 2010).

Tissue Processing and c-Fos Immunohistochemistry

Brains were stored overnight in the fixative (4°C) followed by 3 days in fixative containing 30% sucrose (4°C). Brains were frozen sectioned at 40 μm in the coronal plane and every 6th section (240μm interval) was reacted for c-Fos expression. Additional sections were Nissl-stained to evaluate infusion placements and fornix lesions. For c-Fos immunohistochemistry, floating sections were rinsed in a Tris-buffered (25 mM) saline (TBS) solution, pH 7.4, followed by 20 min in 0.5% H_2O_2 in TBS to quench endogenous peroxidase activity. Additional TBS rinses were followed by 2 hrs in a blocking solution containing 10% normal horse serum and 0.33% Triton X-100 in TBS. Sections were then incubated overnight with a rabbit c-Fos antiserum (PC38, Calbiochem), diluted 1:5000 with the blocking solution. The following day, with intervening TBS rinses, the sections were incubated for 4 hrs with a biotinylated donkey anti-rabbit IgG antiserum (Jackson Immunoresearch), diluted 1:1000 with the blocking solution; and then incubated overnight with an avidin-biotin-peroxidase complex, (ABC Elite, Vector Laboratories), diluted 1:200 with TBS. The next day, sections were reacted with diaminobenzidine as the substrate, enhanced with nickel chloride (Vector Laboratories). Immediately following the reaction, sections were rinsed briefly with ice-cold TBS and mounted on glass microscope slides.

Digital images were acquired and analyzed using equipment and methods previously described (Saint Marie et al., 2006). Images (1200 × 1600 pixels) equivalent to 380×505 μm of tissue area were acquired from 2 regions of the mPFC (infralimbic and prelimbic) and NAC (core and shell) at 3 coronal levels (e.g., Fig. 1A), each separated by ~500 μm (mPFC: +3.2, +2.7, +2.2; NAC: +2.7, +2.2, +1.7; relative to Bregma) based on a standard rat brain atlas (Paxinos and Watson, 1998). For consistency, images of the NAC core were captured midway between the ventral most extent of the lateral ventricle and the dorsal surface of the anterior commissure. Images of the NAC shell were taken from just inside the medial-most curvature of the shell region. Images of the mPFC were oriented to include the cellular (sub-molecular) layers, with those from infralimbic cortex positioned just dorsal to the rhinal incisura and those from prelimbic cortex positioned just ventral to the dorsal extent of the forceps minor of the corpus callosum. Images were corrected for non-uniformities in background illumination and c-Fos+ nuclei were then automatically identified and counted with a macro file written with Image-Pro Plus software (Media Cybernetics) that produced a binary threshold-image of the darkest pixels (gray levels 0–63), split overlapping (dumbbell-shaped) profiles, and filtered objects for size (area ≥ 100 pixels) and roundness [1 ≤ (perimeter^2/(4pi × area)) ≤ 2]. Outlines of acceptable objects were then automatically superimposed on the original image field for editing. Extraneously identified objects, e.g., dirt, were omitted from the final count; and overlapping nuclei that were not split by the filter were added to the count. No stereological-correction formulae were applied in this analysis because the measured objects (c-Fos+ nuclei) were small

(~3.5–7.5 μm diam.) relative to the sampled field (380×505 μm), section thickness (40 μm), and section-sampling interval (~500 μm); and they were consistently sized within brain regions from animal to animal. In addition to the automated nature of the analysis, all histology and image capture, processing, and quantification were performed blind to lesion and drug conditions. Tissue from one side of one level of infralimbic cortex of one (sham lesioned) rat was lost, so the count for this section was imputed; this had no impact on the findings.

Statistical Analysis

Fos data were analyzed by repeated measure ANOVAs for the mPFC and NAC (StatView), using lesion and drug treatment as between subject factors, and side, subregion (mPFC: prelimbic vs. infralimbic cortex; NAC: core vs. shell) and AP level as within subject factors. Post-hoc comparisons were performed with Fisher's Protected Least Significant Difference. Alpha was 0.05.

RESULTS

A summary plot of the VH infusion sites produced in this study is presented in Figure 1B. All but a few of the infusion sites were confined rostro-caudally between −5.8 and −6.3 mm relative to Bregma. Sites clustered near the ventral subicular/CA1 border and many entered the adjacent lateral entorhinal cortex. Occasionally, placements penetrated the caudal extent of the amygdalopiriform transition area of the amygdala. Nissl-stained examples of a normal fornix and one bilaterally lesioned are presented in Figure 1C. The parameters used to produce such lesions (coordinates, current strength and duration) have been shown previously by us to effectively sever the fornix by their ability to block transport of neuroanatomical tracers to and from the ventral hippocampal formation (Saint Marie et al., 2008; Miller et al., 2010).

Examples of anti-c-Fos immunohistochemical staining in the mPFC and NAC, with and without bilateral activation of the VH with NMDA, are presented in Figure 2. The anti-c-Fos staining produced a blue-black reaction product in neuronal nuclei that was elevated in both structures in NMDA-treated cases (see below). In the mPFC, NMDA-induced staining was elevated in all cellular (non-molecular) layers of the cortex and often formed a prominent band of labeled nuclei in the cell-dense layer II. In the NAC, NMDA-enhanced c-Fos expression was less prominent than in the mPFC and staining tended to be more elevated in the shell region compared to the core.

In rats with both fornices intact (n = 30 from experiments A and B), NMDA infusion (0.0 vs 0.8μg/0.5μl/side) had a significant effect on c-Fos expression in both the mPFC (F = 15.85, df 1, 28, p = 0.0004) and the NAC (F = 7.70, df 1, 28, p < 0.01). In the mPFC, there was no significant effect of subregion (F=2.57, df 1,28, ns) or side (F=2.99, df 1,28, ns), but there were significant effects of AP level (F=21.70, df 2,56, p<0.0001) and interactions of AP level × drug (p=0.0005), AP levels × subregion (p<0.0001) and AP level × drug × subregion (p<0.005). This 3-way interaction reflected greater NMDA-stimulated c-Fos expression in rostral vs. caudal infralimbic cortex, but not prelimbic cortex (Fig. 3). In the NAC, there was a significant effect of subregion (F=39.58, df 1,28, p<0.0001): both baseline and drug induced c-Fos expression was significantly higher in the NAC shell vs. the core. There was no significant effect of side (F<1) but there was a significant effect of AP level (F=3.94, df 2,56, p<0.03) and significant interactions of subregion × drug (p<0.009) and subregion × AP level (p<0.001), but not AP level × drug (F<1) or AP level × drug × subregion (F=1.25, df 2,56, ns). The 2-way interactions reflected greater c-Fos expression in the caudal vs. rostral NAC shell but not core, and greater NMDA-stimulated c-Fos expression in the NAC shell vs. core (Fig. 3).

In Experiment B, in which NMDA-stimulated c-Fos expression was compared between rats with bilateral sham (n=22) vs. electrolytic lesions of the fornix (n=26), there was a significant

effect of drug in both the mPFC ($F = 25.87$, df 1, 43, $p < 0.0001$) and NAC ($F = 9.87$, df 1, 41, $p < 0.004$). Within the mPFC, there was no effect of surgery (F<1) or drug × surgery interaction (F<1), suggesting no impact of fornix lesions on overall mPFC NMDA-stimulated c-Fos expression (Fig. 4). ANOVA did detect significant effects of subregion, subregion × AP level, and subregion × drug × AP level, as had been detected among rats with intact fornices (above). Importantly, surgery (sham vs. lesion) did not interact significantly with any drug effects (2-, 3- and 4-way interactions, all p's > 0.20). In contrast, within the NAC, fornix lesions did produce a profound reduction in NMDA-stimulated c-Fos expression in both the core and shell of the NAC (Fig. 4). ANOVA of NAC c-Fos expression revealed a significant effect of surgery ($F = 8.11$, df 1, 41, $p < 0.01$) and a significant drug × surgery interaction (F=4.31, df 1, 41, $p < 0.05$), reflecting the disruption of enhanced NAC c-Fos expression by fornix lesions. As in rats with intact fornices (above), the overall ANOVA of c-Fos expression among sham- and lesion-group rats detected significant effects of NAC subregion and AP level, as well as a drug × subregion interaction (F=12.38, df 1, 41, p<0.002), reflecting greater NMDA-stimulated c-Fos expression in the NAC shell vs. core. There was a significant interaction of surgery × drug × subregion (F=4.99, df 1, 41, p<0.035), reflecting the greater impact of fornix lesions on NMDA effects within the NAC shell vs. core (Fig. 4). Despite this interaction, fornix lesions significantly reduced c-Fos expression after NMDA in both the NAC core (F=6.03, df 1, 23, p<0.025) and shell subregions (F=9.01, df 1, 22, p<0.007).

DISCUSSION

We previously reported anatomical evidence that projections from the VH - particularly the lateral entorhinal cortex - and the embedded olfactory and vomeronasal parts of the amygdala innervate the ventral forebrain via non-fornical routes (Miller et al. 2010). While fiber-tracing studies provide evidence for the anatomical integrity of these projections after fornix lesions, they cannot determine whether these projections remain functionally intact, or more correctly, are activated by intra-VH NMDA infusion. If these non-fornical projections mediate the loss of PPI in fornix-lesioned rats after intra-VH NMDA, then we would expect them to both be functionally intact and activated by NMDA. The present study was designed to assess these possibilities, by examining the impact of intra-VH NMDA infusion on forebrain c-Fos expression after sham vs. electrolytic fornix ablation. As previously reported (Klarner et al. 1998), intra-VH NMDA infusion stimulated c-Fos expression throughout much of the ventral striatum and mPFC. In a clear dissociation, fornix ablation blocked these effects within the NAC, but not within the mPFC. Thus, while both the NAC and mPFC are activated by NMDA infusion into the VH, activation of the NAC but not mPFC is dependent on fornical inputs from the ventral hippocampal formation.

Two issues raised by the present findings deserve comment. First, while NMDA infusion sites were localized primarily within the CA1 and VS, many entered the lateral entorhinal cortex, and this region potently regulates PPI (Swerdlow et al. 2001b) and maintains substantial inputs to the mPFC after fornix lesions (Miller et al. 2010). Thus, the projection from the lateral entorhinal cortex to the mPFC must be considered a likely candidate substrate responsible for both mPFC c-Fos activation and PPI disruption after VH NMDA infusion in fornix-lesioned rats. Second, given the anatomical proximity and infusion volume, it is likely that NMDA activated surrounding tissue, perhaps including portions of the amygdalopiriform transition area of the amygdala. Amygdala activation might stimulate mPFC c-Fos expression via non-fornical fibers either directly or via a potentiation of hippocampal output, but this activation cannot easily be linked to the PPI-disruptive effects of NMDA, because NMDA blockade (rather than stimulation) of the basolateral amygdala (BLA) disrupts PPI (Wan and Swerdlow 1997).

The present findings provide only one line of evidence, which must be interpreted in the context of converging lines of evidence from previous behavioral and anatomical studies. Even in this context, the fact that intra-VH NMDA infusion causes increased mPFC c-Fos expression via non-fornical projections only indirectly suggests that this activation could be causally linked to a loss of PPI. For example, in other brain regions (including the NAC), reductions (rather than increases) in c-Fos expression are associated with reductions in PPI (Saint Marie et al. 2006). Presumably, these differences reflect the nature of the experimental manipulation: enhanced mPFC c-Fos expression after VH NMDA infusion might reflect the NMDA-stimulated release of excitatory amino acids within the mPFC, while reductions in NAC c-Fos expression after low doses of apomorphine might reflect D2-mediated cellular inhibition. Nonetheless, we can only connect mPFC activation and PPI reduction by association and not causality: VH NMDA infusion causes fornix-independent cellular activation in the mPFC, and this activation occurs in a region where lesions block fornix-independent PPI reductions after intra-VH NMDA infusion.

To the degree that we accept these converging lines of evidence, they add credence to the notion that sensorimotor gating is regulated by separable circuits that involve either 1) primarily subcortical elements, e.g. the ventral striatum and its projections to the ventral pallidum (VP) (cf. Swerdlow et al. 2001a; Qu et al. 2009), and 2) primarily cortical elements, e.g. the mesial temporal and medial prefrontal cortices. The fact that these two circuits regulate PPI in a manner that is physiologically separable and perhaps independent is further supported by our ongoing studies using a “disconnection” strategy (serial contralateral manipulations at different circuit levels) (Shoemaker et al. 2005b): disconnection (reduced PPI) can be achieved with serial contralateral cortical manipulations (e.g. VH and mPFC, and VH and BLA) and subcortical manipulations (e.g. NAC and VP), but not with mixed cortical-subcortical manipulations (e.g. VH and NAC).

Conceptually, this pattern of findings suggests that sensorimotor gating – a process whereby the brain regulates the ability of sensory events to inhibit motor responses, and one known to be impaired in several neuropsychiatric disorders – can be controlled independently by anatomically and functionally segregated cortical and subcortical mechanisms. There is clear adaptive value in the ability to successfully inhibit (gate) responses to unwanted or irrelevant information. PPI is a measure of both automatic inhibition (i.e. preconscious, for intervals < 60 ms, which cannot be consciously discerned) and volitional inhibitory processes. The longstanding neural models for the regulation of PPI overlap substantially with those for traditional "reward" circuitry, in which limbic cortical efferents converge with ascending dopamine (DA) projections at the limbic-motor interface within the NAC. Clearly, ascending DA systems regulate some forms of PPI, but the implications of the present line of inquiry is that some or all of the limbic cortical substrates of PPI appear to form a segregated circuit that bypasses the NAC, effecting a change in automatic behavioral inhibition without engaging traditional "reward" circuitry. This segregation of circuits provides a mechanism for “gating” that circumvents control by mesolimbic reward circuitry - a new model to account for a willful / consciously-directed inhibition of a motor response to an impulse. This segregation may be particularly important in certain disorders of impaired sensorimotor gating, including Tourette Syndrome (Castellanos et al. 1996; Swerdlow et al. 2001c), obsessive compulsive disorder (Swerdlow et al. 1993; Hoenig et al. 2005), and perhaps even schizophrenia (Braff et al. 1978; Swerdlow et al. 2006), where patients endeavor to use rational cognitive (cortically-based) tools to willfully inhibit sensations and urges and thoughts that they experience as unwanted and distressing.

In summary, projections from the VH to the mPFC appear to regulate laboratory-based gating measures in a manner that is segregated from circuitry linking the VH with the ventral striatum;

conceivably, this circuitry may contribute to the ability to consciously gate responses to irrelevant or intrusive information.

LIST OF ABBREVIATIONS

BLA	basolateral amygdala
DA	dopamine
mPFC	medial prefrontal cortex
NAC	nucleus accumbens
NMDA	N-methyl-D-aspartate
PPI	prepulse inhibition of startle reflex
TBS	tris-buffered saline
VH	ventral hippocampal region
VP	ventral pallidum

Acknowledgments

This study was supported by NIMH Award MH053484 (NRS).

REFERENCES

Braff D, Stone C, Callaway E, Geyer M, Glick I, Bali L. Pre-stimulus effects on human startle reflex in normals and schizophrenics. Psychophysiology 1978;15:339–343. [PubMed: 693742]

Castellanos FX, Fine EJ, Kaysen D, Marsh WL, Rapoport JL, Hallett M. Sensorimotor gating in boys with Tourette's syndrome and ADHD: preliminary results. Biol. Psychiatry 1996;39:33–41. [PubMed: 8719124]

Graham F. The more or less startling effects of weak prestimuli. Psychophysiology 1975;12:238–248. [PubMed: 1153628]

Hoenig K, Hochrein A, Quednow BB, Maier W, Wagner M. Impaired prepulse inhibition of acoustic startle in obsessive-compulsive disorder. Biol. Psychiatry 2005;57:1153–1158. [PubMed: 15866555]

Klarner A, Koch M, Schnitzler HU. Induction of Fos-protein in the forebrain and disruption of sensorimotor gating following N-methyl-D-aspartate infusion into the ventral hippocampus of the rat. Neuroscience 1998;84:443–452. [PubMed: 9539215]

Miller EJ, Saint Marie RL, Breier MR, Swerdlow NR. Pathways from the ventral hippocampus and caudal amygdala to forebrain regions that regulate sensorimotor gating in the rat. Neuroscience 2010;165:601–611. [PubMed: 19854244]

Mogenson GJ, Nielsen M. A study of the contribution of hippocampal-accumbens-subpallidal projections to locomotor activity. Behav Neural Biol 1984;42:38–51. [PubMed: 6508692]

Paxinos, G.; Watson, C. The Rat Brain in Stereotaxic Coordinates. 4th Edition. San Diego, CA, USA: Academic Press; 1998.

Qu Y, Saint Marie RL, Breier MR, Ko D, Stouffer D, Parsons LH, Swerdlow NR. Neural basis for a heritable phenotype: differences in the effects of apomorphine on startle gating and ventral pallidal GABA efflux in male Sprague-Dawley and Long-Evans rats. Psychopharmacol 2009;207:271–280.

Saint Marie RL, Neary AC, Shoemaker JM, Swerdlow NR. The effects of apomorphine and D-amphetamine on striatal c-Fos expression in Sprague-Dawley and Long Evans rats and their F1 progeny. Brain Res 2006;1119:203–214. [PubMed: 16979142]

Saint Marie, RL.; Miller, EJ.; Breier, M.; Swerdlow, NR. So many roads: Alternate pathways from startle gating-regulatory portions of ventral hippocampus innervate nucleus accumbens and medial prefrontal cortex in rat; Proceedings of the 47th Annual Meeting of the American College of Neuropsychopharmacology; Scottsdale, AR, USA. 2008.

Shoemaker JM, Saint Marie RL, Bongiovanni MJ, Neary AC, Tochen LS, Swerdlow NR. Prefrontal D1 and ventral hippocampal NMDA regulation of startle gating in rats. Neuroscience 2005a;135:385–394. [PubMed: 16125865]

Shoemaker JM, Neary A, Tochen LS, Breier M, Saint Marie RL, Swerdlow NR. Hippocampal-accumbens circuit regulation of startle gating in rats tested via disconnection. Society for Neuroscience Abstracts 2005b:453.3.

Swerdlow NR, Braff DL, Geyer MA, Koob GF. Central dopamine hyperactivity in rats mimics abnormal acoustic startle response in schizophrenics. Biol Psychiatry 1986;21:23–33. [PubMed: 3080033]

Swerdlow NR, Benbow CH, Zisook S, Geyer MA, Braff DL. A preliminary assessment of sensorimotor gating in patients with obsessive compulsive disorder. Biol. Psychiatry 1993;33:298–301. [PubMed: 8471686]

Swerdlow NR, Geyer MA, Braff DL. Neural circuit regulation of prepulse inhibition of startle in the rat: Current knowledge and future challenges. Psychopharm 2001a;156:194–215.

Swerdlow NR, Hanlon FM, Henning L, Kim YK, Gaudet I, Halim ND. Regulation of sensorimotor gating in rats by hippocampal NMDA: anatomical localization. Brain Res 2001b;898:195–203. [PubMed: 11306005]

Swerdlow NR, Karban B, Ploum Y, Sharp R, Geyer MA, Eastvold A. Tactile prepuff inhibition of startle in children with Tourette's syndrome: in search of an "fMRI-friendly" startle paradigm. Biol Psychiatry 2001c;50:578–585. [PubMed: 11690592]

Swerdlow NR, Shoemaker JM, Noh HR, Ma L, Gaudet I, Munson M, Crain S, Auerbach PP. The ventral hippocampal regulation of prepulse inhibition and its disruption by apomorphine in rats are not mediated via the fornix. Neuroscience 2004;123:675–685. [PubMed: 14706779]

Swerdlow NR, Light GA, Cadenhead KS, Sprock J, Hsieh MH, Braff DL. Startle gating deficits in a large cohort of patients with schizophrenia: relationship to medications, symptoms, neurocognition, and level of function. Arch Gen Psychiatry 2006;63:1325–1335. [PubMed: 17146007]

Swerdlow NR, Weber M, Qu Y, Light GA, Braff DL. Realistic expectations of prepulse inhibition in translational models for schizophrenia research. Psychopharm 2008;199:331–388.

Wan FJ, Caine SB, Swerdlow NR. The ventral subiculum modulation of prepulse inhibition is not mediated via dopamine D2 or nucleus accumbens non-NMDA glutamate receptor activity. Eur J Pharmacol 1996;314:9–18. [PubMed: 8957213]

Wan FJ, Swerdlow NR. The basolateral amygdala regulates sensorimotor gating of acoustic startle in the rat. Neuroscience 1997;76:715–724. [PubMed: 9135045]

Witter, MP.; Amaral, DG. Hippocampal formation. In: Paxinos, G., editor. The Rat Nervous System. 3rd Edition. Academic Press; 2004. p. 635-670.

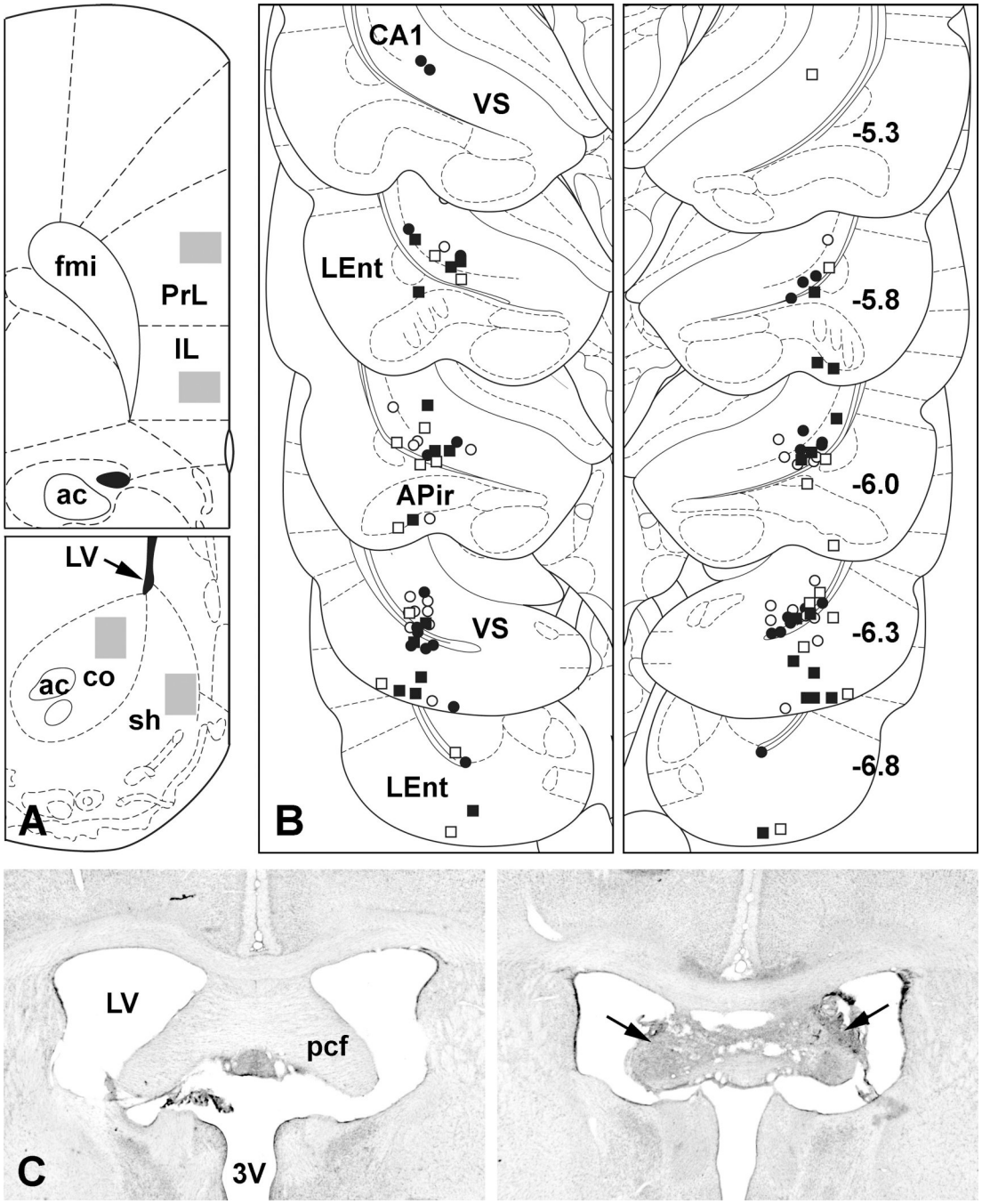

Figure 1.

A. Examples of regions sampled (gray rectangles) for c-Fos-protein expression in infralimbic (IL) and prelimbic (PrL) cortices of the mPFC (Top) and in the core (co) and shell (sh) of the NAC (Bottom). **B**. Summary plot of VH infusion sites: open symbols represent vehicle infusions, filled symbols NMDA infusions; square symbols represent bilaterally lesioned cases, round symbols unlesioned cases. Each side of the bilateral infusions is represented in a separate panel. More rostrally (upper levels), placements are confined primarily to the boundary region of CA1 and ventral subiculum (VS). Some of the more caudal placements (lower levels) can be seen in the lateral entorhinal cortex (LEnt). Occasionally an infusion track penetrates the amygdalopiriform transition area (APir) of the caudal amygdala. Numbers in

the right panel represent A/P levels relative to Bregma. Except for a few outliers, nearly all of the placements were between −5.8 and −6.3 mm. **C**. Nissl-stained examples of the precommissural fornix (pcf) from a case with no fornix lesion (Left) and from one that received bilateral electrolytic lesions (arrows) of the pcf (Right). In this case, only a small amount of tissue appears intact at the midline, and our previous work (Miller et al., 2010) has demonstrated that fibers projecting from the VH pass along the lateral edges of the pcf. 3V, third ventricle; ac, anterior commissure; fmi, forceps minor of the corpus callosum; LV, lateral ventricle. Figures A and B are derived form a standard rat brain atlas (Paxinos and Watson, 1998).

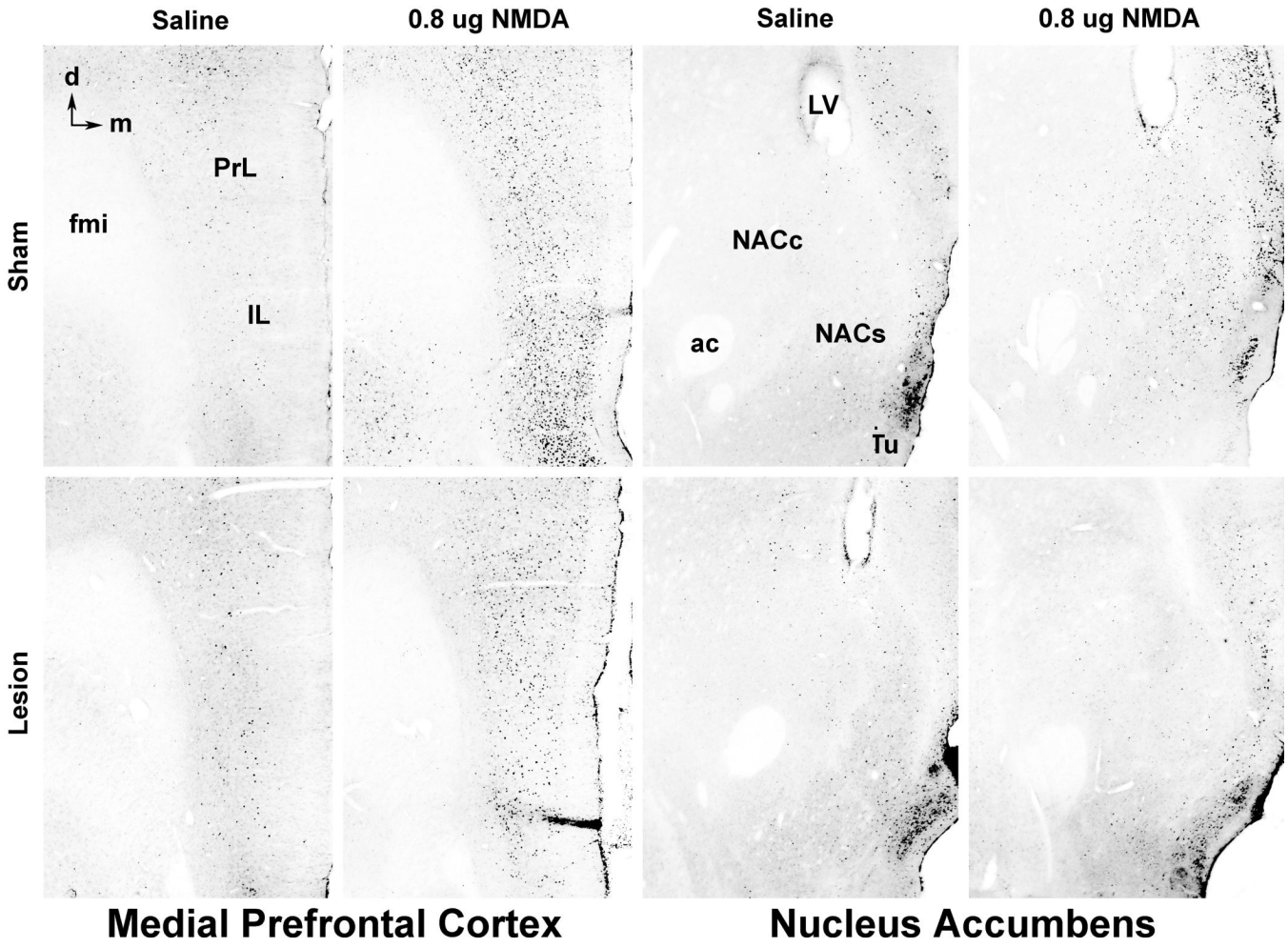

Figure 2.

Examples of c-Fos-protein expression (small black cell nuclei) in the infralimbic (IL) and prelimbic (PrL) cortices of the medial prefrontal cortex (leftmost columns) and in the core (NACc) and shell (NACs) of the nucleus accumbens (rightmost columns) following bilateral saline or NMDA infusion into the VH. VH NMDA infusion leads to enhanced c-Fos expression in both the IL and PrL of the mPFC and in the NAC, especially the NACs, in unlesioned cases (top row). In cases with bilateral fornix lesions (bottom row), VH NMDA-induced c-Fos expression remains high in the IL and PrL, but is largely absent in the NAC. Examples were selected because c-Fos expression in each was near the mean for its group. ac, anterior commissure; d, dorsal; fmi, forceps minor of the corpus callosum; LV, lateral ventricle; m, medial; Tu, tubercle.

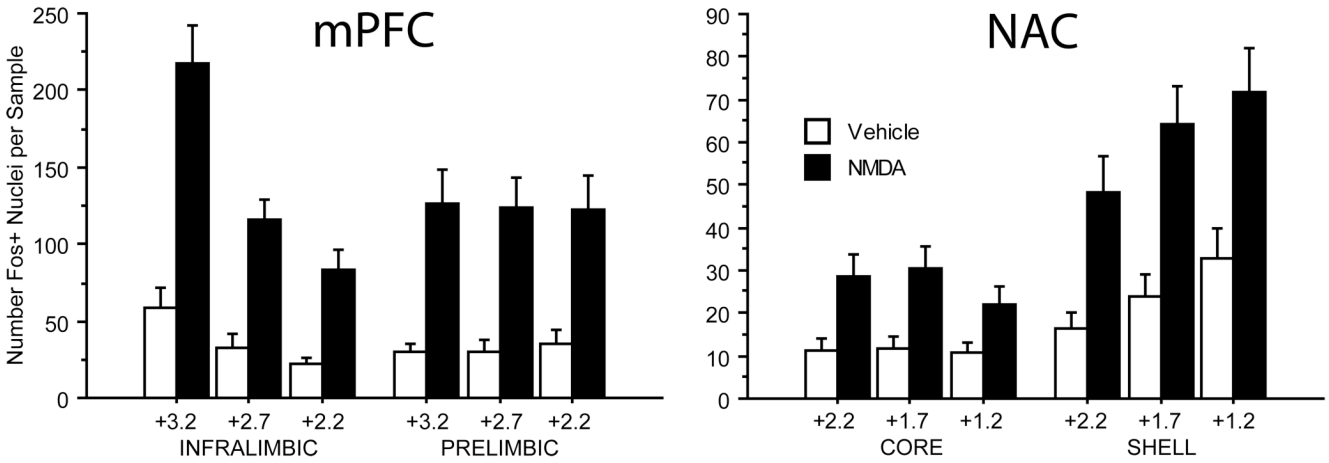

Figure 3.

Summary of c-Fos-protein expression for all unlesioned cases used in this study (n=30). In the mPFC (Left), bilateral VH MNDA infusion significantly elevated c-Fos expresssion in both the infralimbic and prelimbic cortices at all three coronal levels examined (see text for details). Whereas the amount of c-Fos expression did not differ between coronal levels in the prelimbic cortex, c-Fos expression in infralimbic cortex was significantly higher at the most rostral level (+3.2 from Bregma) compared to the other two levels (both $p<0.0001$). Similarly in the NAC (Right), bilateral VH NMDA infusion significantly elevated c-Fos-protein expression in both the core and shell of the NAC at all three coronal levels sampled in each (see text for details). Expression was found to be significantly more elevated in the shell compared to the core ($p=0.0001$), and in the shell there appeared to be a rostral to caudal gradient with c-Fos expression at the most caudal level (+1.2) significantly more elevated than at level +2.2 ($p<0.01$).

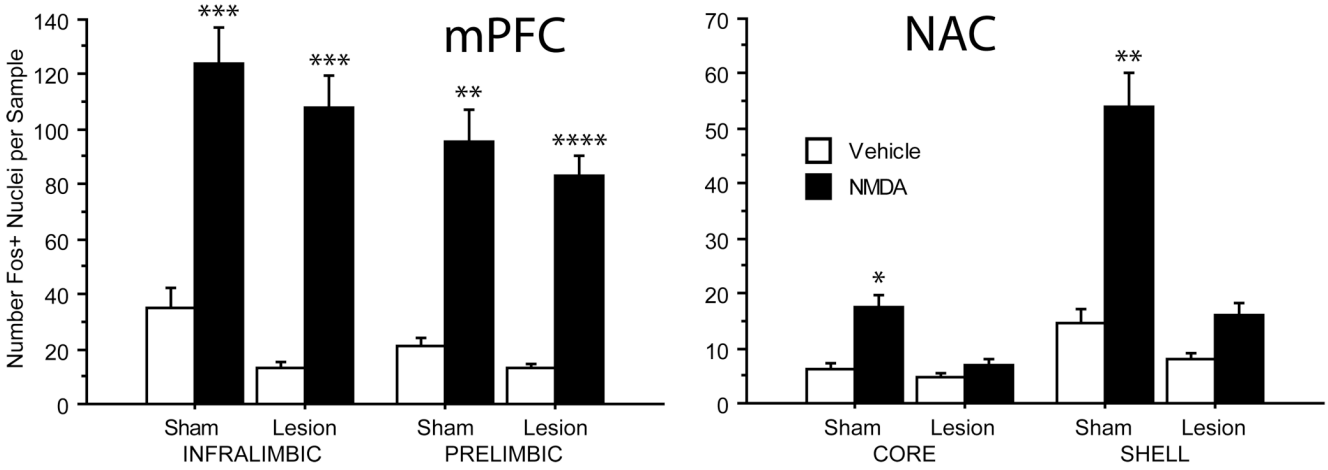

Figure 4.

c-Fos protein expression in unlesioned (sham) cases (n=22) compared to those with bilateral lesions of the fornix (n=26). As described in Figure 3, bilateral NMDA infusion into the VH led to significantly elevated c-Fos expression in the infralimbic and prelimbic cortices of the mPFC (Left) and in the core and shell of the NAC (Right) in unlesioned cases compared to matched cases that received vehicle infusions in the VH. In cases with bilateral fornix lesions, VH NMDA infusion persisted in elevating c-Fos expression in both regions of the mPFC, but had minimal effects on expression in both regions of the NAC compared to cases with vehicle infusions. *$p < 0.05$, **$p < 0.01$, ***$p < 0.005$, ****$p = 0.0002$.